

Supplementary Information

Supplementary Figure Legends

Fig. S1 NRIP expression in the spinal cord and skeletal muscles at 4 and 6 weeks of age in WT and SOD1 G93A mice. **(A)** NRIP expression in the spinal cord at 4 weeks of age in WT and SOD1 G93A mice. Total proteins from L3-L5 spinal cord were subjected to Western blot (WB) analysis for NRIP expression, with GAPDH serving as the loading control. The right panel shows the quantification of NRIP expression conducted through densitometry analysis. **(B)** NRIP expression in the gastrocnemius (GAS) muscles at 4 weeks of age in WT and SOD1 G93A mice. The right panel illustrates the quantification. **(C)** NRIP expression in the tibialis anterior (TA) muscles at 4 weeks of age in WT and SOD1 G93A mice. The right panel displays the quantification. **(D)** NRIP expression in the spinal cord at 6 weeks of age in WT and SOD1 G93A mice. The right panel represents the quantification of NRIP expression. **(E)** NRIP expression in the gastrocnemius (GAS) muscles at 6 weeks of age in WT and SOD1 G93A mice. The right panel illustrates the quantification. **(F)** NRIP expression in the tibialis anterior (TA) muscles at 6 weeks of age in WT and SOD1 G93A mice. The right panel shows the quantification. Each group consisted of N = 3 mice for both WT and SOD1 G93A. Data are presented as mean \pm SEM. Statistical analysis was conducted using the Student t-test. * $P < 0.05$ and ** $P < 0.01$.

Fig. S2 Immunofluorescence analysis of AAV-GFP expression in the spinal cord of WT mice via intramuscular injection. The analysis was conducted on both control WT mice (without AAV-GFP treatment) and WT mice administered with AAV-GFP through intramuscular injection. The spinal cord was dissected into cervical, thoracic, and lumbar segments. Each segment was co-stained with anti-GFP (green, indicating GFP expression) and anti-NeuN (red, a neuron marker) antibodies. DAPI was used as the nuclear stain. Scale bars: 100 μ m.

Fig. S3 Transgene copy number determination in SOD1 G93A mice treated with AAV-NRIP and AAV-GFP. The transgene copy number in SOD1 G93A mice treated with AAV-NRIP and AAV-GFP was determined by real-time PCR. The Δ Ct (cycle threshold) of transgene copy number was assessed by comparing a reference gene (mouse *apob*) with the transgene (human *SOD1*). The AAV-GFP group comprised 3 mice, and the AAV-NRIP group comprised 4 mice. Data are presented as mean \pm SEM. Statistical analysis was performed using the Student t-test. ns, no significance.

38

39 **Fig. S4** Total distance moved and rearing frequency of SOD1 G93A mice with AAV-
40 GFP or AAV-NRIP treatment in males and females. (A) The total distance moved by
41 SOD1 G93A mice with AAV-GFP or AAV-NRIP treatment was recorded from 100 to
42 147 days using EthoVision Video Tracking Software (Noldus) during a 10-minute test.
43 The total distance traveled in the box was measured. In the male group, data are
44 presented as mean \pm SEM. * P =0.045 at the age of 126 days; ns, no significance; one-
45 way ANOVA with Tukey's post hoc test. In the female group, data are presented as
46 mean \pm SEM. * P =0.0496 at the age of 120 days; ns, no significance; one-way ANOVA
47 with Tukey's post hoc test. (B) Rearing frequency, indicating the frequency of mice
48 standing on their hindlimbs in the box, was recorded from 100 to 147 days. In the male
49 group, data are presented as mean \pm SEM. * P =0.0166 at the age of 126 days; ns, no
50 significance; one-way ANOVA with Tukey's post hoc test. In the female group, data
51 are presented as mean \pm SEM. * P =0.0381 at the age of 120 days; * P =0.0429 at the
52 age of 133 days; ns, no significance; one-way ANOVA with Tukey's post hoc test.

53

54 **Fig. S5** Therapeutic effects of AAV-NRIP on rotarod performance and grip force via
55 intramuscular injection in SOD1 G93A mice. (A) Evaluation of AAV-NRIP efficacy
56 in rotarod performance of SOD1 G93A mice at the age of 120 days. Mice were placed
57 on a rotating rod set at 20 rpm, and the time until falling was recorded. N=6 for each
58 group. (B) Analysis of grip force. Forelimb strength was measured five times for each
59 mouse at the age of 120 days. N=6 for each group. Data are presented as mean \pm SEM.
60 Statistical analysis was conducted using the Student t-test. ns, no significance. (C)
61 Kaplan-Meier survival curves comparing AAV-NRIP-treated and AAV-GFP-treated
62 SOD1 G93A mice. Statistical differences were analyzed using the Logrank test. ns, no
63 significance.

64

65 **Fig. S6** AAV-NRIP gene therapy improves ChAT and NeuN co-positive MN survival
66 in SOD1 G93A mice. (A) Quantification of total ChAT⁺/NeuN⁺ MN numbers per spinal
67 anterior horn in WT mice (N=4) and SOD1 G93A mice treated with AAV-GFP (N=4)
68 and AAV-NRIP (N=4). Data are presented as mean \pm SEM. ** P =0.0026 (WT vs.
69 SOD1 G93A+AAV-GFP); ** P =0.0036 (SOD1 G93A+AAV-GFP vs. SOD1
70 G93A+AAV-NRIP); one-way ANOVA with Tukey's post hoc test. (B) Quantification
71 of ChAT⁺/NeuN⁺ MN numbers with a cell size smaller than 500 μ m² per spinal
72 anterior horn in WT mice (N=4) and SOD1 G93A mice treated with AAV-GFP (N=4)
73 and AAV-NRIP (N=4). Data are presented as mean \pm SEM. Statistical analysis was
74 conducted using the one-way ANOVA with Tukey's post hoc test. ns, no significance.

Figure S1

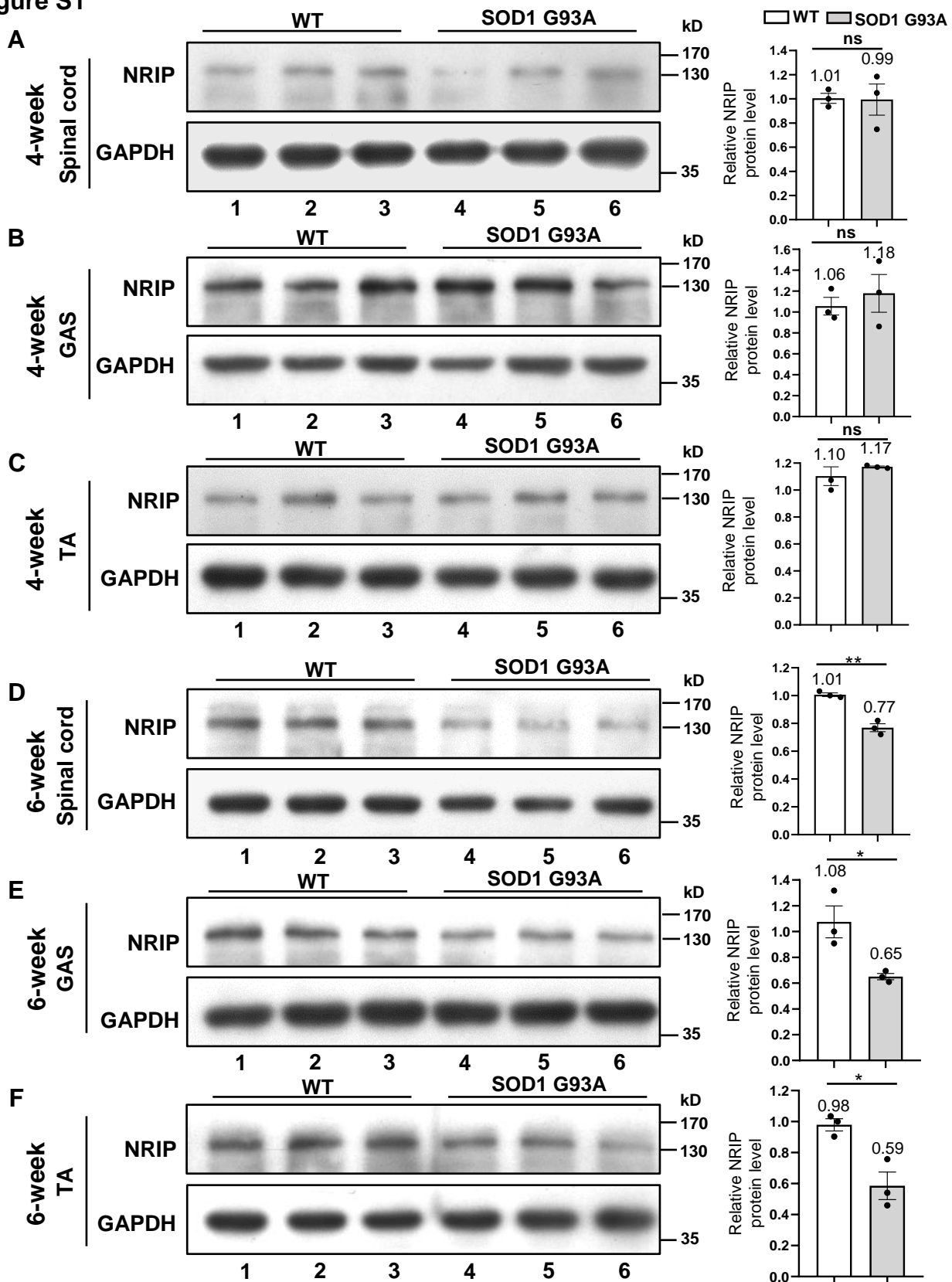


Figure S2

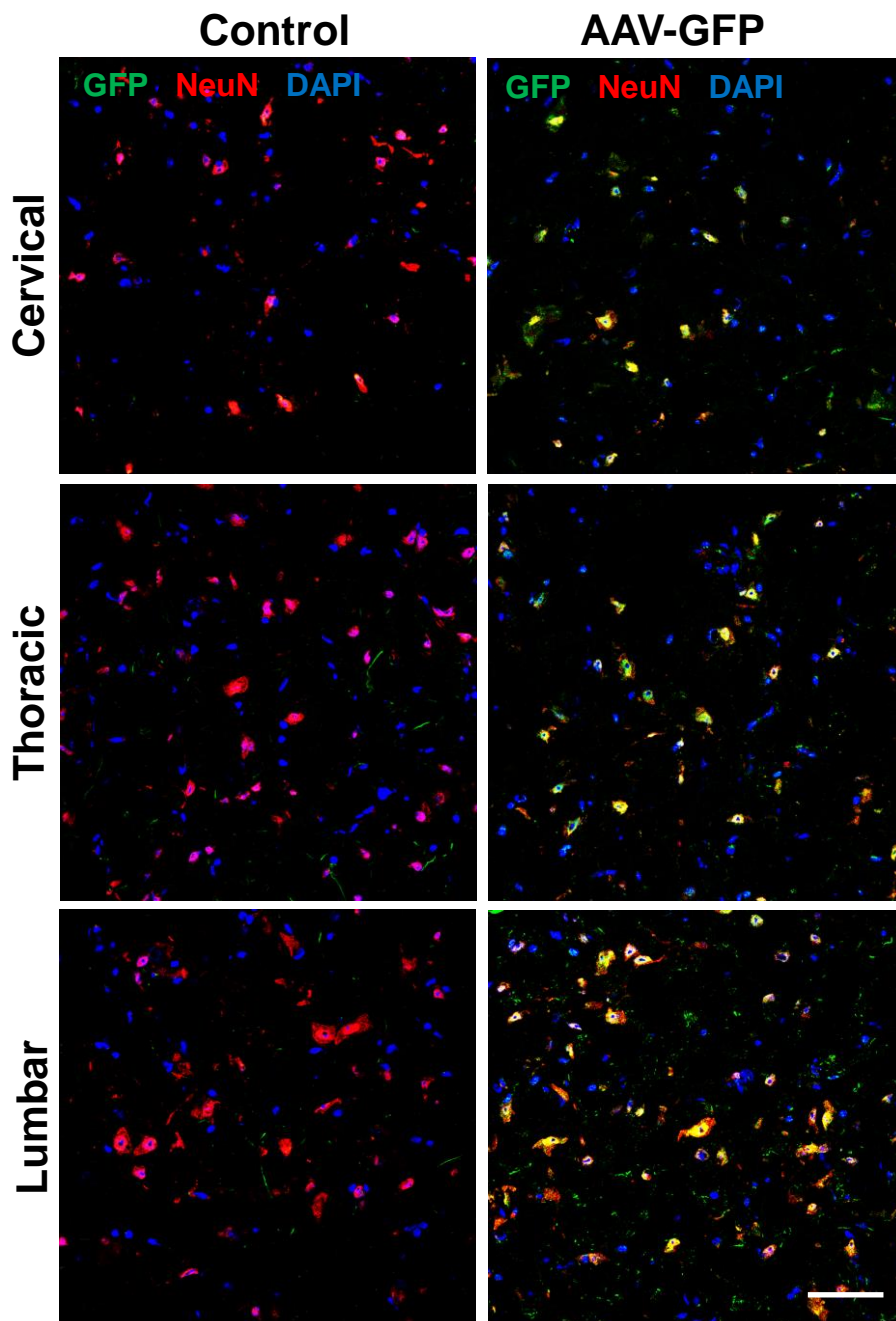


Figure S3

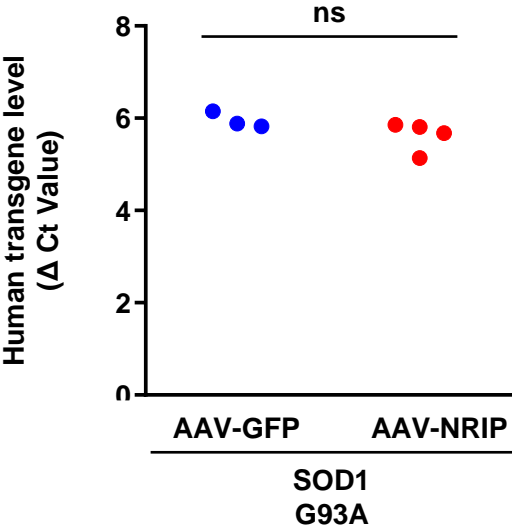
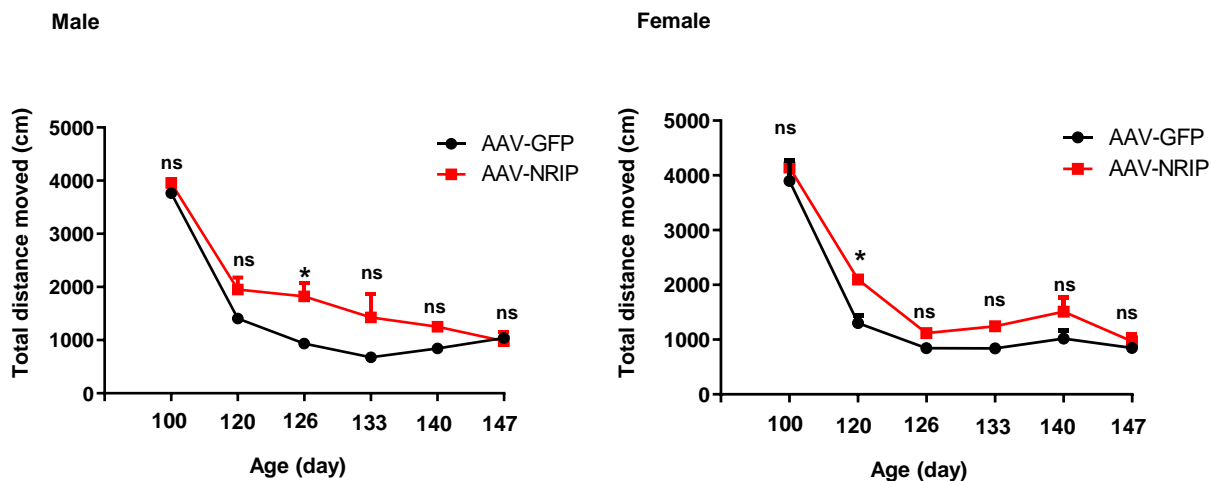


Figure S4

A



B

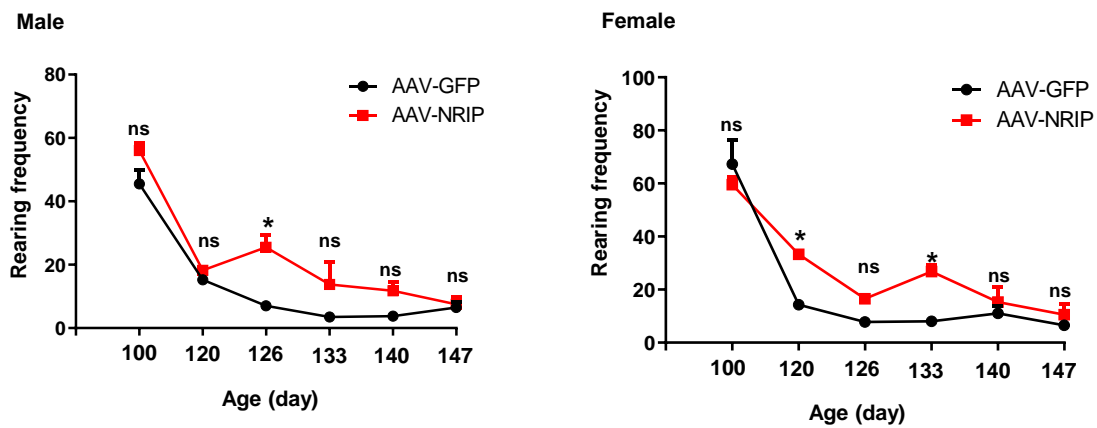
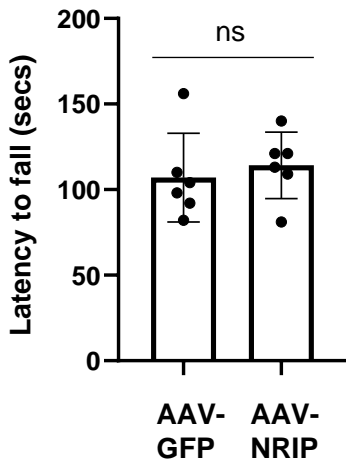
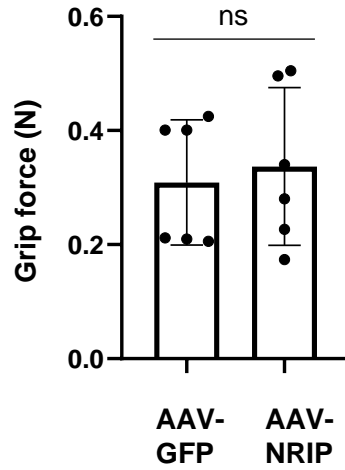


Figure S5

A



B



C

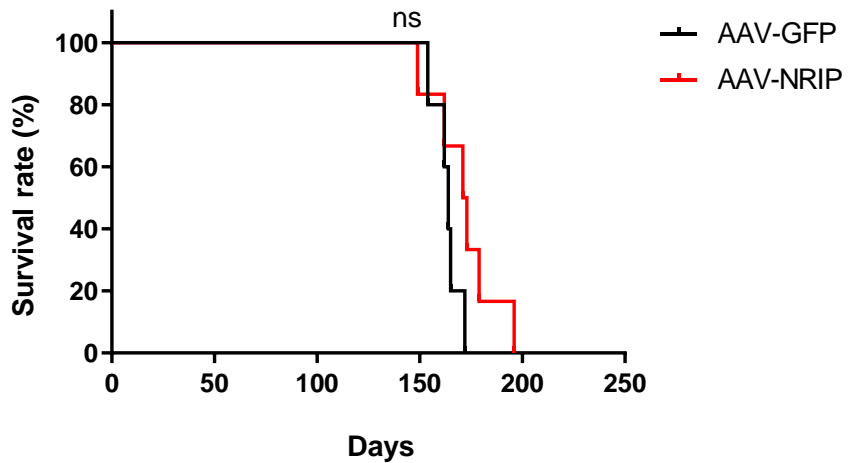
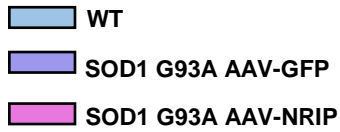
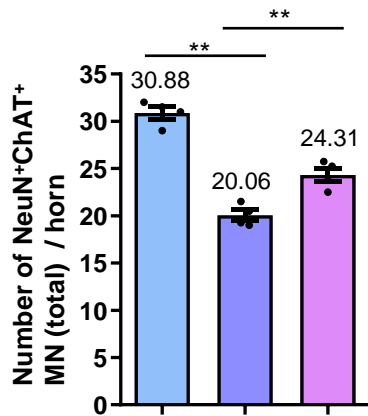


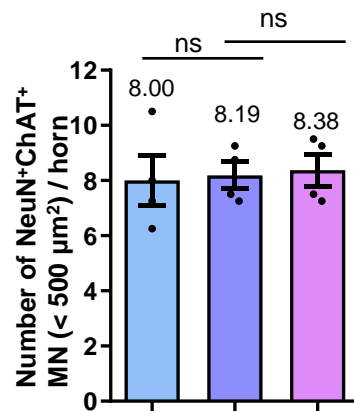
Figure S6



A



B



Supplementary Information

Grayscale images of Fig.1D, Fig. 2C, Fig. 2D, Fig. 4A, Fig. 4D, Fig. 5A, Fig. 6A and Fig. S2

Figure 1D
Grayscale

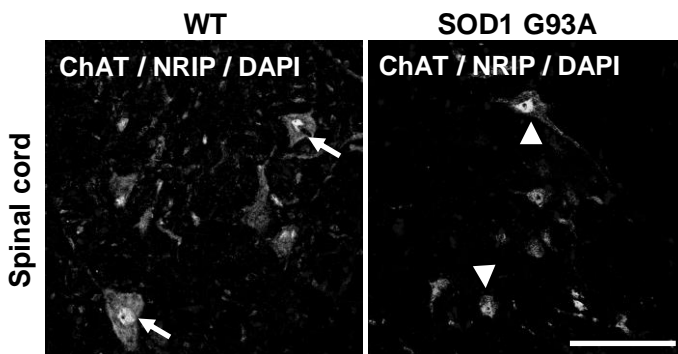


Figure 2C
Grayscale

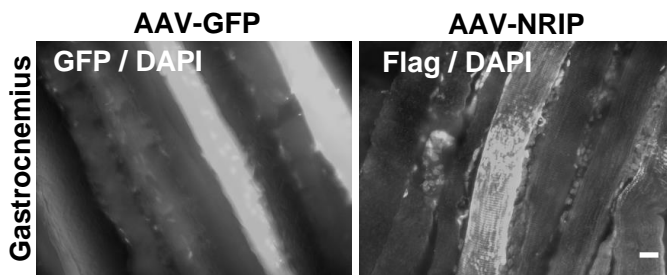


Figure 2D
Grayscale

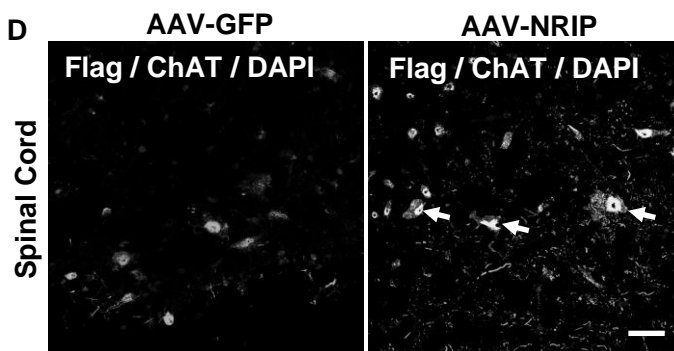


Figure 4A
Grayscale

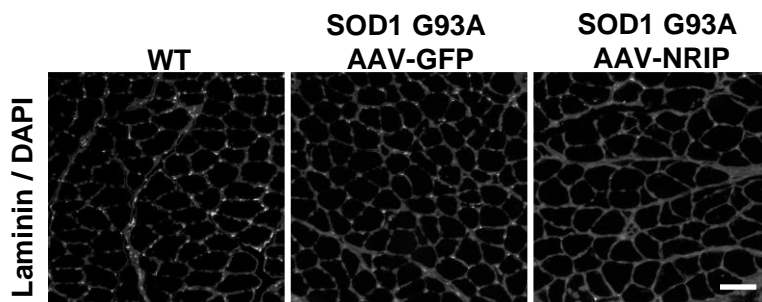


Figure 4D
Grayscale

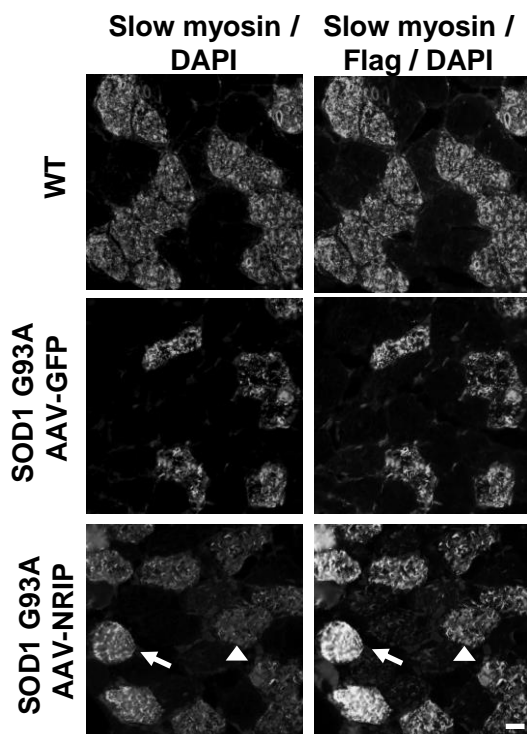


Figure 5A
Grayscale

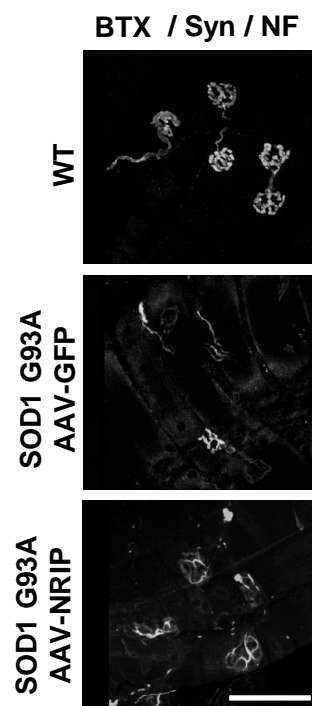


Figure 6A
Grayscale

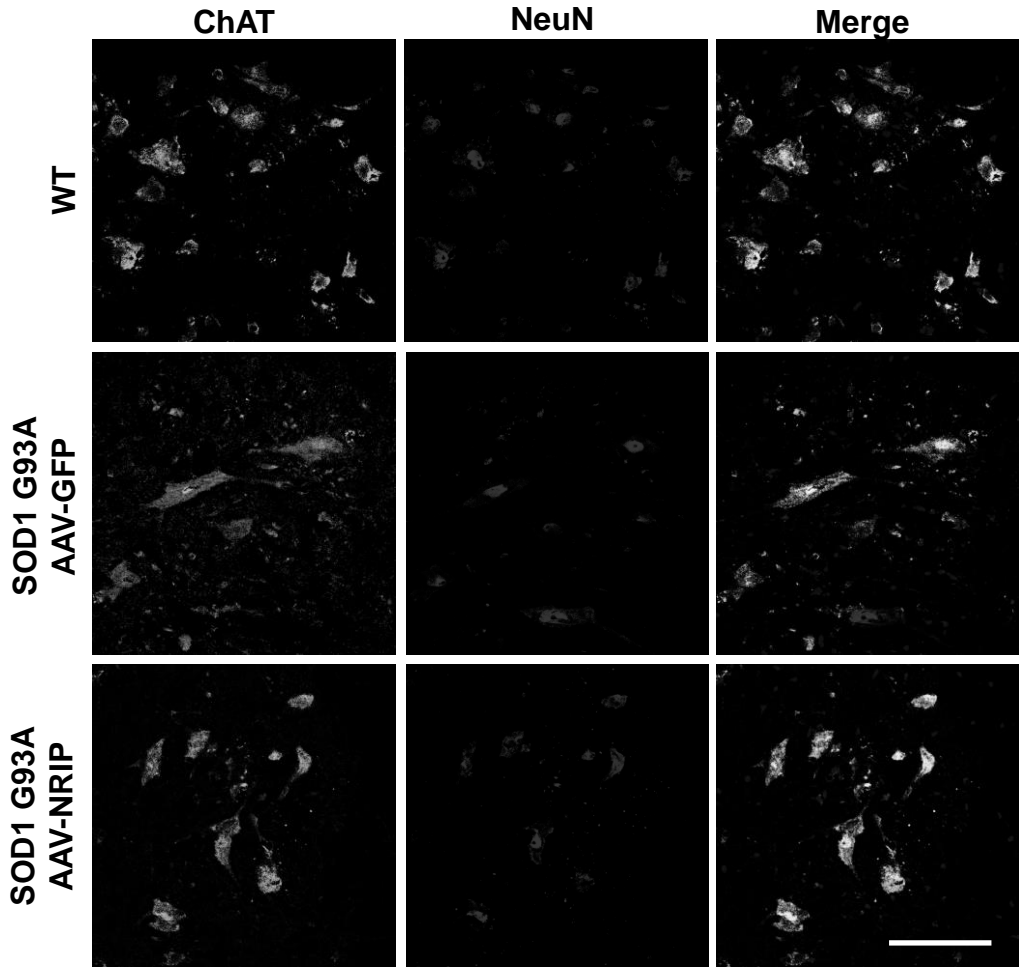


Figure S2
Grayscale

